Journal of Optoelectronics and Advanced Materials Vol. 5, No. 3, September 2003, p. 777 - 785

THE ROLE OF TiO IN THE PEROVSKITE NUCLEATION AND (111) ORIENTATION SELECTION IN SOL-GEL PZT LAYERS

F. Vasiliu*, G. J. Norga[a], L. Fe[b], D. Wounters[b], D. Van der Biest[c]

National Institute of Materials Physics, P. O. Box MG-7, R-76900, Bucharest-Magurele, Romania
[a]IBM Zurich Research Laboratory, Saumerstrasse 4, CH 8803 Ruschlikon, Switzerland
[b]IMEC, Kapeldreef 75, B-3001 Leuven, Belgium
[c]Ku-Leuven, MTM Department, Kastelpark, B-3001, Leuven, Belgium

We have proposed a lattice matching mechanism for the selection of (111) PZT orientation, based on the experimental evidence of the formation of cubic TiO on the Pt electrode surface in the earlier stages of thermal processing of PZT layers .Thus, a fitting of TiO with Pt and, consequently of PZT (Ti-rich) with TiO (orientation relationship:*TiO (111)//Pt(111) and respectively PZT (111)//TiO(111)*) has been evaluated. Similar mismatch degree values were obtained comparatively with the classical cases of intermetallic layer "templates" (for example Pt_xPb, Pt_3Ti,etc). The very good lattice matching supports the proposed mechanism, consisting in the formation of cubic TiO on Pt and, later, of the nucleation and growth of PZT (tetragonal) of cubic TiO, where is formed. In comparison with the case of TiO_2(rutile) matching, previously proposed by other groups,having larger mismatch values,the cube-to-cube orientation relationship could explain the selection of (111) orientation as a major one in some specific conditions affected by some parameters especially related to solution chemistry and thermal processing steps.

(Received July 4, 2003; accepted July 31, 2003)

Keywords: Sol-gel, Ferroelectric layers, Microtexture, Transmission electron microscopy, Orientation relationship

1. Introduction

PZT nucleation and texture appeared to be controlled by the electrode system and the interface properties. (111) textured Pt electrodes have favoured a high degree (111) orientation of PZT layers but other different orientations could be obtained on Pt (111) [1].

The essential role of Ti, TiO_x or TiO_2, played in the nucleation of the perovskite phase was underlined previously [2-4].The initial presence of Ti, TiO_x or TiO_2 on the Pt surface or appearance of Ti or Ti oxides at Pt/PZT interface, due to Ti diffusion through Pt and later oxidation in the case of Pt/Ti electrodes, have a crucial role in the orientation selection of PZT layers.

For sol-gel layers, <111> texture of PZT was obtained by using nanometer thick Ti layers [2], TiO_2 films on Pt films [1], TiO_x films on Pt [5] or after the TiO_x layer occurrence on Pt surface in Pt/Ti –electrode system [4].In the first case, even a lowering of PZT crystallization temperature at 460 ^oC was obtained as compared to the case of template layer absence. However, highly (100)-oriented PZT films could be also crystallized, for similar compositions and experimental parameters, on TiO_2 and $PbTiO_3$ seed layers [6].

These different conclusions seemed to be related to the oxidation degree of Ti present or diffused on Pt surface, the crystallization degree of Ti oxides and the thermal budget and atmosphere used for bottom electrodes and PZT layers thermal treatments.Also, the deposition method and

* Corresponding author: fvasiliu@alpha1.infim.ro

solution chemistry have also an essential role in the evaluation of Ti oxides involvement in PZT nucleation and orientation selection.

For sputtered PZT layers on TiO_2 seed films, the $PbTiO_3$ texture could be turned from (100) to (111) orientation [7]. However, the authors have observed that TiO_2 is effective only when it is ordered before nucleation starting and a strong evidence for a strained rutile (110) structure is observed and, thus, the matching with perovskite structure increased.

The aim of this work is to propose a mechanism for the selection of <111> orientation based on the earlier formation of cubic TiO oxide in the pyrolisis or in the first steps of the PZT crystallization.

2. Experimental

The Pt/Ti electrodes were prepared using RF sputtering deposition of 10 nm Ti followed by 100 nm Pt on thermally oxidized (100) Si wafers. The reactive Pt/Ti stack was subsequently stabilized by rapid thermal annealing (RTA) at 700 ^oC for 5 minutes in O_2.The resulting layers are columnar with a strong (111) fiber texture.

A PZT precursor solution with Zr/Ti ratio 30/70, was deposited by spin coating onto the preannealed Pt/Ti bottom electrodes. To compensate for Pb evaporation during thermal treatment, a Pb excess of 15% with respect to the stoichiometric amount was added. Three layers were deposited, resulting in a total film thickness of approximately 200 nm, with the pyrolysis step carried out after each layer on a temperature controlled hot plate. In our experiments, we studied the effect of varying pyrolysis temperature (between 350 and 450 °C), pyrolysis duration (10 s or 2 min), as well as the effect of a preliminary drying step at 200 ^oC. The crystallization treatment of the layers was always performed at 600 °C, 30 min on hot plate in air.

TEM, SAED and EDX investigations were performed by means of a Philips CM-30 electron microscope. Plan view and cross section specimens were prepared by the usual dimpling and ion milling techniques or by using FIB.

3. Experimental results

In Fig. 1, a typical cross section of a PZT layer subjected to drying (200 ^oC, 2 min) and a short time pyrolisis (350 ^oC, 10 sec) is shown. Since after crystallization treatment (600 ^oC, 30 min), PZT layer has a highly <111> orientation, the formation of an intermediate layer (Pt_3Ti, Pt_xPb) could be expected. Ti layer, initially present at the limit Pt/SiO_2 was vanished by diffusion, especially through Pt grain boundaries, to the Pt surface. EDX analysis has shown the presence of Ti and some small amounts of Pb and Pt in the interfacial layer formed at the PZT/Pt interface.

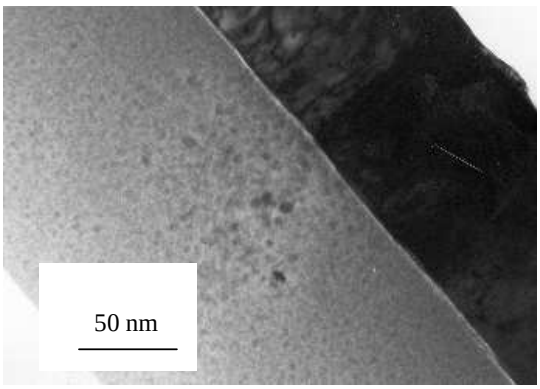

Fig. 1. Cross section TEM image of a PZT layer subjected to drying (200 ^oC, 2 min) and to a short pyrolisis (350 ^oC, 10 s).

SAED patterns of some areas, observed in plan view for the same sample, showed the presence of some faint rings of a nanocrystalline pyrochlore (Fig. 2) accompagnied by the occurrence of two rings (d = 2.10 Å and d = 2.40 Å) of a new crystallized phase which could be TiO (space group Fm3m-225) having a lattice parameter a = 4.17 Å (JCPDS file no. 8-0117). The cubic TiO oxides having the same structure exhibit a lattice constant varying, probably as a function of oxygen stoichiometry degree, between 4.17-4.29 Å. Since the strongest lines of Pt occurred for d=2.25 Å and d=1.95 Å, no possible overlapping would be expected in our case for a relatively thick PZT layer.

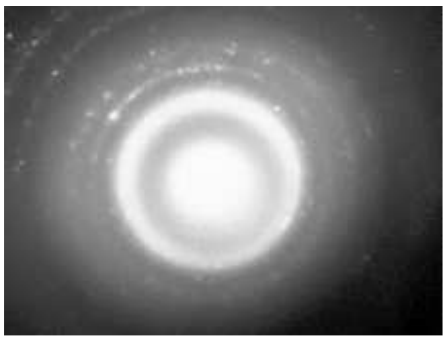

Fig. 2. SAED pattern of the same specimen from Fig. 1, observed in plan view, allowing the detection of weak rings of nanocrystalline pyrochlore and of two rings of cubic TiO.

Also, the main rings associated to Pt_xPb or Pt_3Ti are not very far localized but a good distinction could be made. Moreover, in the areas containing a very well crystallized pyrochlore, these two rings, associated to cubic TiO disappeared (Fig. 3), suggesting an important role of this compound, formed after pyrolisis at Pt interface, in the intermediate phase crystallization and perovskite nucleation.

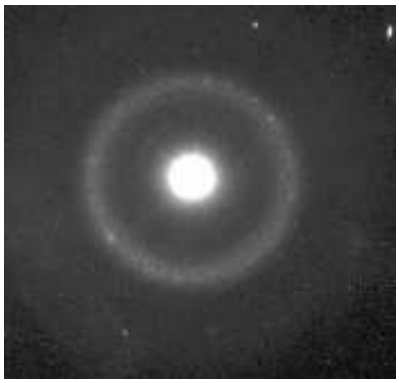

Fig. 3. SAED pattern showing the vanishing of cubic Ti O rings and the presence of a perovskitic or intermediate phase with a weak crystallization.

For the same specimen, but in cross section, bright and corresponding dark field images (Fig. 4a and Fig. 4b), taken with the strongest spot (111) of Pt, have confirmed the presence of some grains limited by [110] walls. Simultaneously, there are many small grains having 7-12 nm grain size) out in the interfacial layer, formed at the PZT/Pt limit (the PZT layer was in this area sweeped out due to the ion milling preparation), which appeared as reflecting particles. Taking into account also the EDX results, we supposed that the objective aperture has included not only the Pt diffraction spot for dark field imaging but also the very close weaker spot (200) of TiO (I=100) (d_{200}^{TiO} = 2.12 Å; d_{111}^{Pt} = 2.25 Å). In a plan view specimen of a PZT layer , subjected only at pyrolisis at 450 ^oC, 2 min, without drying) out, SAED patterns contains besides of a quasi-amorphous ring of intermediate fluorite-like phase) out, and a very weak ring of the strongest line of TiO_2 but also some spots of relatively strong

intensity associated to cubic TiO (Fig. 5). However, a coherent and indexable pattern of cubic TiO was not found.

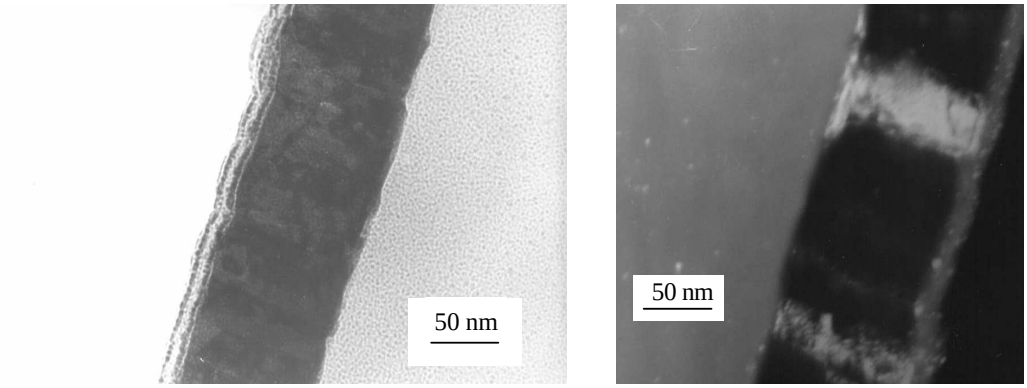

a b

Fig. 4. (a) Bright field image of a PZT layer deposited on Pt ; (b) Dark field image of the same area, imaged by means of (111) Pt and cubic TiO (200) spots

Fig. 5. SAED pattern of a PZT layer observed in plan view, subjected only at a a pyrolisis step (450 ^{o}C, 2 min), without drying. Besides the quasi-amorphous ring of an intermediate fluoritic phase and the very weak ring associated to TiO_2, some strong spots of cubic TiO are present.

On the other part, in many SAED patterns of PZT layers subjected to the crystallization treatment, the strongest rings of TiO_2 (rutile) were detected either in plan view but also in cross section samples.

For the case of a PZT layer, subjected to drying (200 ^{o}C, 2 min), pyrolisis (350 ^{o}C, 10 s) and annealing (600 ^{o}C, 30 min) and having a very good <111> orientation, a thin layer of about 20 nm thickness was observed between PZT and Pt layers. Excepting some contamination elements related to specimen preparation (Cu, Si), EDX analysis evidenced only the presence of Ti and a small Pb amount. It is interesting that, although TiO was expected to have only a transient role in pyrolisis stage, a SAED pattern of this annealed specimen, associated to PZT/Pt interface, evidenced the occurrence of the strongest three lines (d_{111} = 2.47 Å; d_{200} = 2.14 Å; d_{220} = 1.52 Å) of cubic TiO (a= 4.29 Å) but, in the first case, an overlapping with (101) TiO_2 line was possible.

Many references [8-11] have reported the detection by EDX, AES, RBS of the presence of Ti oxides in and over Pt grains, after the bottom electrode annealing. This evidence is cited as to be related to TiO_{2-x} oxides but, unfortunately, the exact oxidation state was not found.

Sreenivas et al [11] have shown that, besides rutile TiO_2, in Pt/Ti bilayer metallization may be present various phases with the general non-stoechiometric formula of TiO_{2-x} and that the driving force for the Ti diffusion is the formation of a reduced oxide at the interface. Also, encapsulation of a

Pt film by a thin layer of TiO_{2-x} has been reported by Sun et al [12] and was attributed to the diffusion of O_2 and Ti-O through the Pt grain boundaries.

A very comprehensive analysis of the oxidation state of Pt/Ti bottom electrode [13] has shown that, even for short thermal treatments at 650 ^oC in oxygen, the O/Ti ratio decreases very rapidly on a depth of about 20 nm from the initial hypotetical value 2 on the Pt surface. In a layer, inside Pt grains, of about 40 nm thickness, the ratio O/Ti is constant, having a value of about 1.2. This is the stability range of α-$Ti_{1-x}O$, which represents a low temperature modification of TiO (β) [14]. Finally, in the last 30-40 nm of Pt layer, in the stability range of TiO (α) phase, according to the equilibrium diagram Ti-O [15], the decrease of the O/Ti ratio is drastic.

4. Model

Therefore, we suggest that the cubic TiO, resulted from an incomplete oxidation of diffused Ti from the Pt/Ti bottom electrode on the Pt surface, has a crucial role , starting from the initial pyrolisis and/or in the first stages of annealing, in the selection of <111> orientation of PZT layers. A very good lattice matching of TiO with Pt and of PZT (especially Ti-rich) with TiO could be estimated (Figs. 6-8). In the last case , the mismatch degree has similar values as compared to the case of intermetallic template layers (Pt_xPb [16], Pt_3Ti [17], etc).

In comparison with TiO_2 (rutile) case, having a worser mismatch, in each case a cube-to-cube orientation relationship: TiO(111)// Pt(111) and PZT (111)// TiO(111) respectively, could be expected.

From Fig. 6, which show the possible orientation relationship between (111) TiO planes and (111) Pt planes, some observations are evident:
-the mismatch degrees of TiO with (111) Pt are: $\Delta d_{[011]} = +5.4\%$ si $\Delta d_{[211]} = 6.0\%$
-a comparison of the fittings existing for cube-to-cube orientation relationship TiO(111)//Pt(111) with the corresponding one of TiO_2 (rutile) reveals that in the last case the mismatch degrees of TiO_2 with Pt(111) [13] are similar or larger comparative to the case of TiO:

$TiO_2(100)//Pt(111) \rightarrow (\Delta d_{001} = 6.8\%; \Delta d_{010} = -4.3\ \%)$
$TiO_2(110)//Pt(111) \rightarrow (\Delta d_{001} = 6.8\%; \Delta d_{2/3\,[110]} = -9.8\ \%)$

In Fig. 7, we have evaluated the fitting degrees of (111) PZT ("Ti planes") with (111) to planes. For the lattice matching of PZT with TiO and respectively Pt, the results are the following:

$PZT(111)//TiO(111) \rightarrow (\Delta d_{[011]} = -1.7\%;\ \Delta d_{[211]} = -2.5\ \%)$
$PZT\ (111)//Pt(111) \rightarrow (\Delta d_{[011]} = +3.8\%;\ \Delta d_{[211]} = +3.8\ \%)$

whereas in the case of the lattice matching of (111) PZT to TiO_2(and also , as a comparison, to RuO_2), the results are:

$PZT\ (111)\ //TiO_2(110)\ (PZT\ [011]//TiO_2[001];PZT[211]//TiO_2[110]) \rightarrow$
$(\Delta d_{[011]} = -2.7\%;\ \Delta d_{[211]} = +15.0\ \%)$

$PZT\ (111)\ //TiO_2(100)\ (PZT\ [011]//TiO_2[001];PZT[211]//TiO_2[010]) \rightarrow$
$(\Delta d_{[011]} = -2.7\%; \Delta d_{[211]} = +8.5\ \%)$

and respectively:

$PZT(111)//RuO_2(100)\ (PZT[011]//RuO_2[001];PZT[211]//RuO_2[010]) \rightarrow$
$(\Delta d_{[011]} = -8.0\%;\ \Delta d_{[211]} = +10.6\ \%)$

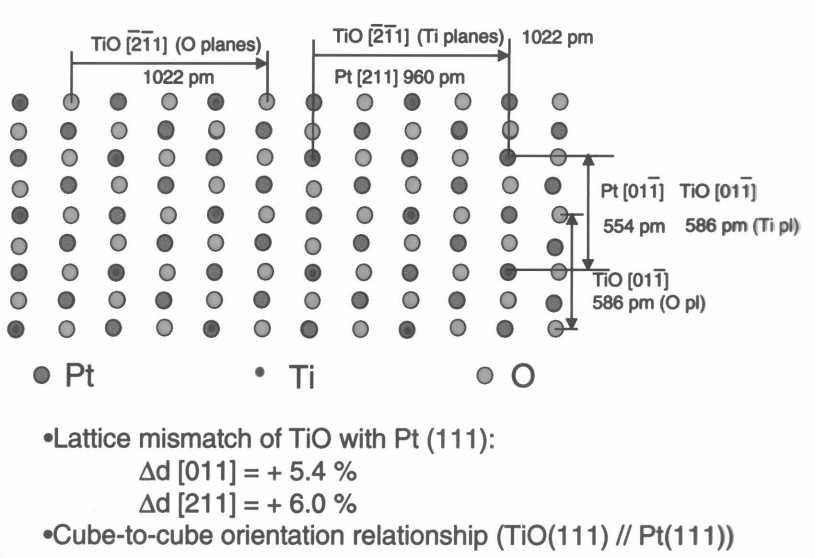

Fig. 6. Possible orientation relationship between (111) TiO planes and (111) Pt planes.

Finally, in Fig. 8 is shown the epitaxial relationship between (111) PZT planes ("PbO_3" planes) and cubic TiO (111) planes. The evaluation results of the mismatch degree are the following:

PZT(111)//TiO(111)→ ($\Delta d_{[011]}$ = -1.7%;$\Delta d_{[211]}$ = -2.5%)
PZT(111)//Pt(111)→ ($\Delta d_{[011]}$ = +3.8 %;$\Delta d_{[211]}$ = +3.8%)

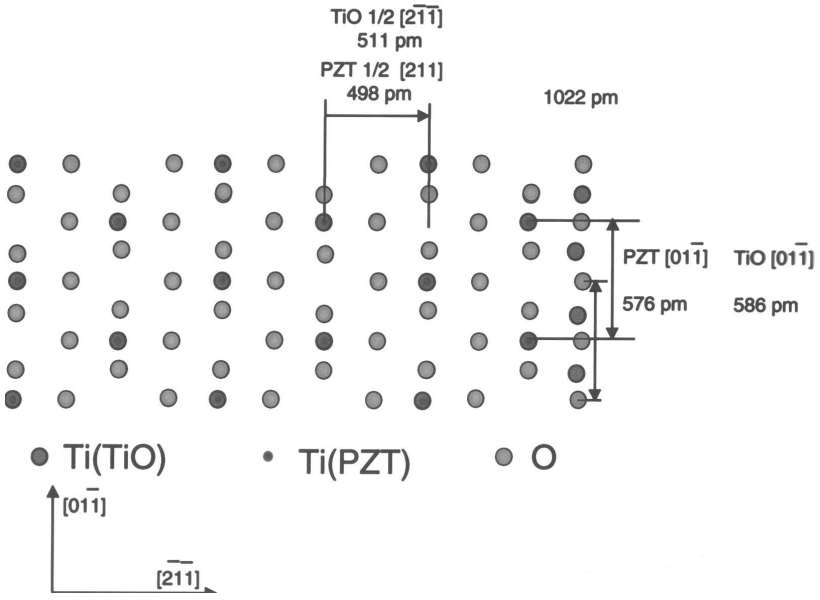

Fig. 7. (111) PZT planes ("Ti" planes) on (111) TiO planes.

These values are much lower (indicating a more perfect epitaxial relationship) than in the case of the relationship wth TiO_2, respectively RuO_2:

PZT(111) //TiO_2 (110) (PZT [011] //TiO_2 [001]; PZT [211] // TiO_2 [110])→
($\Delta d_{[011]}$ =-2.7%;$\Delta d_{[211]}$ =+15.0%)

PZT(111)//TiO_2(100) (PZT [011] //TiO_2 [001]; PZT [211] // TiO_2 [010]) →
($\Delta d_{[011]}$ =-2.7%;$\Delta d_{[211]}$ =+8.5%)

and, respectively:

PZT(111)//RuO_2(100) (PZT[011] // RuO_2 [001];PZT [211] //RuO_2 [010]) →
($\Delta d_{[011]}$ =-8.0 %;$\Delta d_{[211]}$ =+10.6 %)

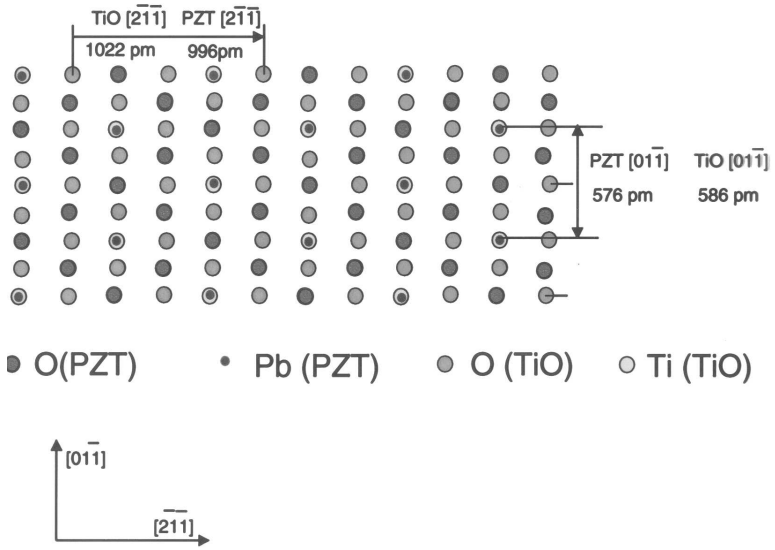

Fig. 8. (111) PZT planes (PbO_3 planes) on (111) TiO planes.

5. Discussion

For short time and/or low temperature of pyrolisis and thermal annealing, eventually coupled with a reducing atmosphere(used for annealing or created at the Pt/PZT interface due to the solution chemistry [18], the presence of cubic TiO appears as a very important factor which promote <111> PZT texture.In many cases, when it is claimed the importance of the presence of TiO_{2-x} or TiO_2 for to promote <111> orientation, initially present as seeds or formed during earlier stages of thermal treatments of PZT layers, it would be possible that a very thin TiO layer (formed on Pt grains at the interface with PZT) to be responsible for the orientation selection.
The presence of oriented TiO_2 layers or a mixing of TiO_{2-x} (x > 1)and TiO_2 (eventually amorphous) could lead to <100> texture or random orientation. In fact, for higher temperature and long time annealing, oxidizing annealing atmospheres or for oxidizing conditions at the interface PZT/Pt, especially during drying or pyrolisis, these last two textures will be prevalent.

Although the (100) PZT planes have the lowest activation growth energy, the existence of a good lattice matching between crystalline TiO and PZT will decrease the high active nucleation energy of PZT. The nucleation on the cubic TiO will mainly yield thus <111>-oriented perovskite grains. In the case of the presence of TiO_2 islands or films on Pt grains, the texture will be finally dominated by <100> orientation. The presence of an amorphous layer of Ti oxides or a mixing of small particles of various Ti oxides, having different structures could leaded to a random orientation. All these facts are also sustained by the lack of direct influence of Pt<111> oriented layer in the <111> orientation selection.

It is very important to emphasize that these conclusions could be valid only for sol-gel PZT layers and for Ti-rich compositions. Other mechanisms for the orientation selection could be

operational for other physical deposition methods (sputtering, laser ablation,etc) and for Zr-rich compositions. This statement could easily explain the texture change of the sputtered $PbTiO_3$ from (100) to (111) orientation by adding 1-5 nm thick TiO_2 layers, having a strained rutile (100) structure [7] or the orientation control provided for Zr-rich compositions by using of some template layers [6]. Even for the same Zr/Ti ratio and deposition method, the pyrolisis treatment and solution chemistry could be decisive, fact which can explain the reported existence [16,17] or the absence of some intermetallic layers in various cases.

Therefore, we have proposed a lattice matching mechanism for the selection of (111) PZT orientation , based on the experimental evidence of the formation of cubic TiO on the Pt electrode surface in the earlier stages of thermal processing of PZT layers. The cube-to-cube orientation relationship could explain the selection of (111) orientation as a major one in some specific conditions affected by some parameters especially related to solution chemistry and thermal processing steps [18].

6. Conclusions

1) Some "lattice matching" models have been developed in order to explain the selection of some preferential orientation on a given substrate. TEM, HREM, SAED and EDX measurements have pointed out the of current formation of substoichiometric TiO_{2-x} oxides on the Pt surface electrode during the sol-gel PZT thermal processing. In this aim, we have proposed a fitting ("lattice matching") of TiO with Pt and, consequently, of PZT (Ti-rich) with TiO. In the last case, the deviation degree from an ideal fitting ("mismatch') has similar values comparatively with the classical cases of intermetallic layer "templates" (for example Pt_xPb, Pt_3Ti,etc)

In comparison with the case of TiO_2(rutile) matching, previously proposed by other groups,having larger mismatch values, it would be expected in each case a cube-to-cube orientation relationship: *TiO (111)//Pt(111) and PZT (111)//TiO(111) respectively*.

The very good lattice matching supports the proposed mechanism, consisting in the formation of cubic TiO on Pt and, later, of the nucleation and growth of PZT (tetragonal) or cubic TiO.

2) The proposed "lattice matching" relationships suggests the following orientation selection mechanism for sol-gel PZT layers:

-nucleation on cubic TiO oxide yields mainly <111> oriented perovskitic grains

-when TiO_2 islands or films are presented on the Pt surface, the final texture will be dominated by the <100> orientation.

References

[1] K. G. Brooks, I. M. Reaney, R. D. Klissurska, Y. Huang, L. Bursill, N. Setter, J. Mater. Res. **9**, 2540 (1994).
[2] K. Aoki, Y. Fukuda, K. Humata, A. Nishiamura, Jpn. J. Appl. Phys. **34**, 192(1995).
[3] T. Hase, T. Sakuma, K. Amanuma, T. Mori, A. Ochi, Y. Migasoka, Integr. Ferroelectrics **8**, 89 (1995).
[4] G. J. Willems, D. J. Wouters, H. E. Maes, Micr. Engineering **29**, 217 (1995).
[5] G. Velu, T. Haccart, D. Remiens, Integr. Ferroelectrics **23**, 1 (1998).
[6] R. E. Koritala, M. T. Lanagan, N. Chen, G. R. Bai, Y. Huang, S. K. Streiffer, J. Mater. Res. **15**, 1962 (2000).
[7] P. Muralt, T. Maeder. L. Sagalowicz, S. Hiboux, S. Scalese, D. Naumovic, R. G. Agostino, N. Xantopoulos, H. J. Mathieu, L. Patthey, E. L. Bullock, J. Appl. Phys. **83**, 3835 (1998).
[8] C. S. Hwang, M. D. Vaudin, P. K. Schenck, J. Mater. Res. **13**, 368 (1998).
[9] R. Bruchhaus, D. Pitzer, O. Eibl, U. Scheithauer, W. Hoesler, in "Ferroelectric Thin Films II ", ed. By A. I. Kingon, E. R. Myers, B. A. Tuttle (MRS Symp. Proc. 243, Pittsburgh, PA, 1992) pp. 123-128.
[10] J. O. Olowolafe, R. E. Jones, A. C. Campbell, P. D. Manias, R. L. Hedge, C. J. Mogab, in "Ferroelectric Thin Films II", ed. By A. J. Kingon et al (MRS Symp. Proc. 243, Pittsburgh,

PA, 1992) pp. 355-360.
[11] K. Sreenivas, I. Reaney , T. Maeder, N. Setter, C. Jagadish, R. G. Elliman, J. Appl. Phys. **75**, 232 (1994).
[12] Y. M. Sun, D. N. Belton, J. M. White, J. Phys. Chem., **90**, 5178 (1986).
[13] T. Maeder, Ph. D. Thesis, Lausanne, EPFL, 1997.
[14] H. Matzke, "Diffusion in nonstoichiometric oxides", in "Nonstoichiometric oxides", pp. 155-232, ED. By O. T. Sorensen, Acad. Press, New York (1981).
[15] W. G. Moffatt, ed., "The Handbook of Binary Phase Diagrams", 1-2, General Electric, Schenectady, New York, USA (1976-82).
[16] S. Y. Chen, I-Wei Chen, J. Appl. Phys. **77**, 2332 (1994); **77**, 2337 (1994).
[17] T. Tani, Z. Xu, D. A. Payne, MRS Symp. Proc. **310**, 269 (1990).
[18] L. Fe, G. Norga, D. Wouters, R. Nouwen, L. C. Van Poucke, J. Sol-Gel Sc. and Technol. **19**, 149 (2000).